

Dynamics of inertial active particles in a microchannel with Poiseuille flow

Harshita Tiwari and Sanket Biswas

(GCT/1940097 and GCT/1940108)

under the supervision of

Dr. Kamlesh Kumari

Department of Chemical Engineering
SLIET Longowal

and the joint external supervision of

Dr. Shubhadeep Mandal and Dr. Aloke Kumar

Department of Mechanical Engineering
IISc Bengaluru

May 19, 2023



Contents

1 Introduction

2 Mathematical framework

3 Numerical simulation framework

4 Trajectories and phase spaces

5 Statistical analysis



Introduction

Background

- Active Brownian Particles (ABP) convert free energy from their environments into persistent motion.
- Active motion is observed at both microscopic and macroscopic scales, ranging from birds and insects to colloids and bacteria.
- ABPs use different propulsion mechanisms to move in fluids, often experiencing dynamic environments and confinements.
- They often experience dynamic fluid environments and confinements, and studying their dynamics has numerous applications in several fields.
- The study of their dynamics has promising applications in microfluidic drug delivery, pollutant localization, biofilm formation prevention, microplastic degradation, and mixing.

Motivation

- Previous studies have investigated the behavior of ABPs in microchannels with a Poiseuille flow and the transport properties of chiral ABPs in the same environment.
- Understanding how particle and fluid inertia affects the unsteady propulsion of larger ABPs can lead to the effective design of biomedical devices.



Overview of our research

Progress so far

- ① Conducted a literature review to identify and define the problem statement.
- ② Extended the mathematical model of non-inertial ABP in Khatri and Burada [1] to incorporate particle inertia.
- ③ Developed the corresponding governing equations of motion (EOMs).
- ④ Performed full-scale numerical simulations in MATLAB and COMSOL.
- ⑤ Studied the stochastic dynamics of particle motion, both analytically and numerically.

Possible future work

- ① Verify and validate the model through lab-scale microfluidic experiments.
- ② Extend the model to other complex confined fluidic domains.



Mapping of COs and POs

Our project maps the program objectives (POs) and course objectives (COs) as follows:

POs & COs	PO1	PO2	PO3	PO4	PO5	PO6	PO7	PO8	PO9	PO10	PO11	PO12	PSO1	PSO2
CO1	S	S	W	S	S	M	S	S	S	S	M	M	M	S
CO2	S	S	S	S	S	S	M	S	S	S	M	M	M	S
CO3	S	M	M	S	S	M	S	S	S	S	M	M	M	S



Contents

1 Introduction

2 Mathematical framework

3 Numerical simulation framework

4 Trajectories and phase spaces

5 Statistical analysis



Geometrical setup

- Spherical microswimmer of radius R in 2D;
- Rectangular microchannel with Poiseuille flow:

$$\mathbf{v}_f = v_f \left(1 - \frac{4y^2}{L^2} \right) \hat{\mathbf{e}}_x, \quad (1)$$

L : height of the channel, v_f : centre-line flow speed;

- Channel walls located at $y = \pm L/2$;
- Corresponding vorticity is given by

$$\omega_s = \frac{4v_f y}{L^2}. \quad (2)$$

- Swimmer has mass m and moment of inertia J ;
- $\mathbf{r} = (x, y)$: centre-of-mass position, θ : orientational angle, $\mathbf{n} = (\cos \theta, \sin \theta)$: orientation vector, v_0 : self-propelled speed, Ω : active rotational velocity.
- Swimmer undergoes Brownian diffusion with translational diffusion coefficient

$$D_T = \frac{k_B T}{\gamma} \text{ (Einstein relation),} \quad (3)$$

and rotational diffusion coefficient

$$D_R = \frac{k_B T}{\gamma_R}, \quad (4)$$

k_B : Boltzmann constant, T : temperature, $\gamma = 6\pi\mu R$: translational friction coefficient, μ : fluid viscosity, $\gamma_R = 8\pi\mu R^3$: rotational friction coefficient.

Equations of motion (EOM)

- Neglecting all external forces, the translational motion of the swimmer:

$$\dot{\mathbf{r}} = \mathbf{v}, \quad (5a)$$

$$m\dot{\mathbf{v}} = \gamma(\mathbf{v}_f - \mathbf{v}) + \gamma\sqrt{2D_T}\xi + \gamma v_0\mathbf{n}, \quad (5b)$$

$\gamma(\mathbf{v}_f - \mathbf{v})$: friction force, $\gamma\sqrt{2D_T}\xi$: thermal force, $\gamma v_0\mathbf{n}$: active force, ξ : Gaussian white noise.

- Similarly, the rotational motion:

$$\dot{\theta} = \omega, \quad (6a)$$

$$J\dot{\omega} = \gamma_r(\omega_s - \omega) + \gamma_r\sqrt{2D_R}\eta + \gamma_r\Omega, \quad (6b)$$

$\gamma_r(\omega_s - \omega)$: friction torque, $\gamma_r\sqrt{2D_R}\eta$: stochastic torque, $\gamma_r\Omega$: active torque, η : Gaussian white noise.

- Component-wise EOM:

$$\frac{dx}{dt} = v_x, \quad \frac{dy}{dt} = v_y, \quad \frac{d\theta}{dt} = \omega, \quad (7a)$$

$$\tau \frac{dv_x}{dt} = -v_x + v_f \left(1 - \frac{4y^2}{L^2}\right) + \sqrt{2D_T}\xi_x + v_0 \cos \theta, \quad (7b)$$

$$\tau \frac{dv_y}{dt} = -v_y + \sqrt{2D_T}\xi_y + v_0 \sin \theta, \quad (7c)$$

$$\tau_R \frac{d\omega}{dt} = -\omega + \frac{4v_f y}{L^2} + \sqrt{2D_R}\eta + \Omega, \quad (7d)$$

$\mathbf{v} = (v_x, v_y)$ and $\xi = (\xi_x, \xi_y)$.

Typical times and non-dimensionalisation

- Three typical times characterizing this model:

$$\tau_P = \frac{1}{D_R}, \quad \tau_R = \frac{J}{\gamma_r}, \quad \tau = \frac{m}{\gamma}, \quad (8)$$

τ_P : persistence time, τ_R : orientational relaxation time, and τ : translational relaxation time.

- Dimensionless variables:

$$X = \frac{x}{L}, \quad Y = \frac{y}{L}, \quad T = \frac{v_0 t}{L}, \quad V_x = \frac{v_x}{v_0}, \quad V_y = \frac{v_y}{v_0}, \quad \text{and} \quad \chi = \frac{L\omega}{v_0}.$$

- Dimensionless parameters:

$$D_t = \frac{D_T}{Lv_0}, \quad D_r = \frac{LD_R}{v_0}, \quad V_f = \frac{v_f}{v_0}, \quad \text{and} \quad \mathcal{M} = \frac{L\Omega}{v_0}.$$

- Dimensionless EOM:

$$\frac{dX}{dT} = V_x, \quad \frac{dY}{dT} = V_y, \quad \frac{d\theta}{dT} = \chi, \quad (9a)$$

$$\frac{dV_x}{dT} = -\alpha \left[V_x - V_f(1 - 4Y^2) - \sqrt{2\kappa D_t} \xi_x - \cos \theta \right], \quad (9b)$$

$$\frac{dV_y}{dT} = -\alpha \left[V_y - \sqrt{2\kappa D_t} \xi_y - \sin \theta \right], \quad (9c)$$

$$\frac{d\chi}{dT} = -\beta \left[\chi - 4V_f Y - \sqrt{2\kappa D_r} \eta - \mathcal{M} \right], \quad (9d)$$

$$\alpha = \kappa/\tau, \quad \beta = \kappa/\tau_R, \quad \kappa = L/v_0.$$

Contents

- 1 Introduction
- 2 Mathematical framework
- 3 Numerical simulation framework
- 4 Trajectories and phase spaces
- 5 Statistical analysis



Finite difference equations (FDEs)

- The set of FDEs can be obtained from Eqn. (9) by carrying out the following substitutions:

$$X \rightarrow X_i, Y \rightarrow Y_i, \theta \rightarrow \theta_i; \quad (10a)$$

$$V_x \rightarrow V_{x,i}, V_y \rightarrow V_{y,i}, \chi \rightarrow \chi_i; \quad (10b)$$

$$\frac{dX}{dT} = \frac{X_{i+1} - X_i}{\Delta T}, \quad \frac{dY}{dT} = \frac{Y_{i+1} - Y_i}{\Delta T}, \quad \frac{d\theta}{dT} = \frac{\theta_{i+1} - \theta_i}{\Delta T}; \quad (10c)$$

$$\frac{dV_x}{dT} = \frac{V_{x,i+1} - V_{x,i}}{\Delta T}, \quad \frac{dV_y}{dT} = \frac{V_{y,i+1} - V_{y,i}}{\Delta T}, \quad \frac{d\chi}{dT} = \frac{\chi_{i+1} - \chi_i}{\Delta T}; \quad (10d)$$

$$\xi_x = \frac{w_{x,i}}{\sqrt{\Delta T}}, \quad \xi_y = \frac{w_{y,i}}{\sqrt{\Delta T}}, \quad \eta = \frac{w_{\theta,i}}{\sqrt{\Delta T}}. \quad (10e)$$

(10) $w_{x,i}, w_{y,i}, w_{\theta,i}$: uncorrelated sequences of random numbers with zero mean and standard deviation 1.

- Resulting FDEs:

$$X_{i+1} = X_i + V_{x,i}\Delta T, \quad (11a)$$

$$Y_{i+1} = Y_i + V_{y,i}\Delta T, \quad (11b)$$

$$\theta_{i+1} = \theta_i + \chi_i\Delta T, \quad (11c)$$

$$V_{x,i+1} = V_{x,i} - \alpha\Delta T \left[V_{x,i} - V_f(1 - 4Y_i^2) - \sqrt{2\kappa D_t/\Delta T} w_{x,i} - \cos \theta_i \right], \quad (11d)$$

$$V_{y,i+1} = V_{y,i} - \alpha\Delta T \left[V_{y,i} - \sqrt{2\kappa D_t/\Delta T} w_{y,i} - \sin \theta_i \right], \quad (11e)$$

$$\chi_{i+1} = \chi_i - \beta\Delta T \left[\chi_i - 4V_f Y_i - \sqrt{2\kappa D_r/\Delta T} w_{\theta,i} - \mathcal{M} \right]. \quad (11f)$$

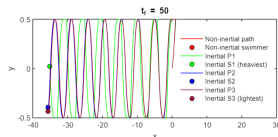


Contents

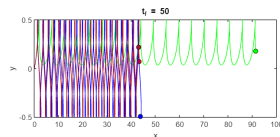
- 1 Introduction
- 2 Mathematical framework
- 3 Numerical simulation framework
- 4 Trajectories and phase spaces
- 5 Statistical analysis



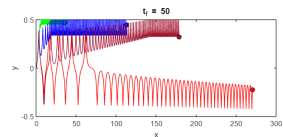
Trajectories: varying flow velocity and temperature
 $(\theta_0 = \pi/6)$



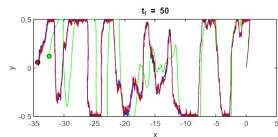
(a) $T = 0\text{K}$, $V_f = 0.28$, $\theta_0 = \pi/6$



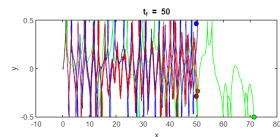
(b) $T = 0\text{K}$, $V_f = 2.25$, $\theta_0 = \pi/6$



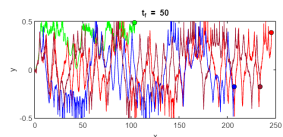
(c) $T = 0\text{K}$, $V_f = 6.75$, $\theta_0 = \pi/6$



(d) $T = 400\text{K}$, $V_f = 0.28$, $\theta_0 = \pi/6$



(e) $T = 400\text{K}$, $V_f = 2.25$, $\theta_0 = \pi/6$

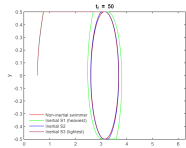


(f) $T = 400\text{K}$, $V_f = 6.75$, $\theta_0 = \pi/6$

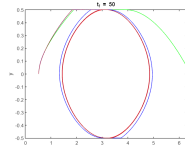
Figure: Trajectories of four active Brownian particles with different masses in a microchannel with Poiseuille flow, subjected to varying non-dimensional flow speeds and temperatures. The trajectories, colored red (Non-inertial path), green (Inertial P1), blue (Inertial P2), and dark red (Inertial P3), correspond to the non-inertial particle and particles with mass $m = 1.5 \times 10^{-8}$ kg (Inertial S1), $m = 1.5 \times 10^{-9}$ kg (Inertial S2), and $m = 1.5 \times 10^{-10}$ kg (Inertial S3), respectively, initial condition: $(X_0, Y_0, \theta_0) = (0, 0, \pi/6)$.



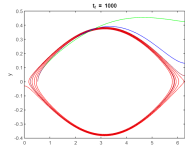
Phase spaces: varying flow velocity and temperature

$$\theta_0 = \pi/6$$


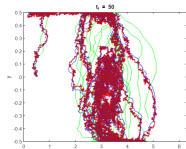
(a) $T = 0\text{K}$, $V_f = 0.28$



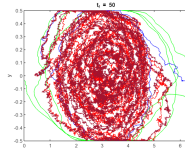
(b) $T = 0\text{K}$, $V_f = 2.25$



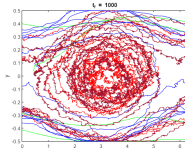
(c) $T = 0\text{K}$, $V_f = 6.75$



(d) $T = 400\text{K}$,
 $V_f = 0.28$



(e) $T = 400\text{K}$,
 $V_f = 2.25$



(f) $T = 400\text{K}$,
 $V_f = 6.75$

Figure: Phase portraits of four active Brownian particles with different masses in a microchannel with Poiseuille flow, under varying non-dimensional flow speeds and temperatures. The red, green, blue, and dark red plots correspond to the non-inertial particle and particles with masses of $1.5 \times 10^{-8} \text{ kg}$ (Inertial S1), $1.5 \times 10^{-9} \text{ kg}$ (Inertial S2), and $1.5 \times 10^{-10} \text{ kg}$ (Inertial S3), respectively, initial condition: $(X_0, Y_0, \theta_0) = (0, 0, \pi/6)$.

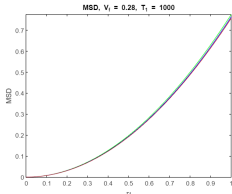


Contents

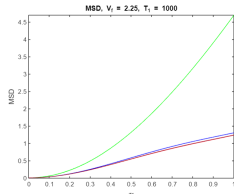
- 1 Introduction
- 2 Mathematical framework
- 3 Numerical simulation framework
- 4 Trajectories and phase spaces
- 5 Statistical analysis



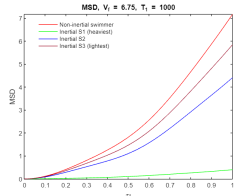
Mean squared displacement (MSD): $\theta_0 = \pi/6$



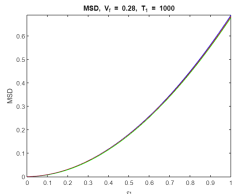
(a) $T = 0\text{K}$, $V_f = 0.28$



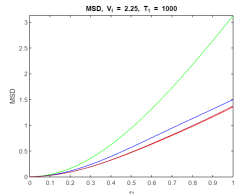
(b) $T = 0\text{K}$, $V_f = 2.25$



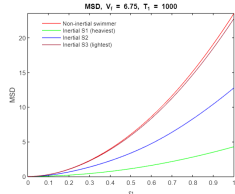
(c) $T = 0\text{K}$, $V_f = 6.75$



(d) $T = 300\text{K}$, $V_f = 0.28$



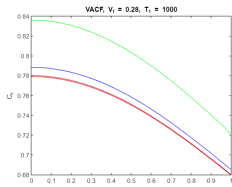
(e) $T = 300\text{K}$, $V_f = 2.25$



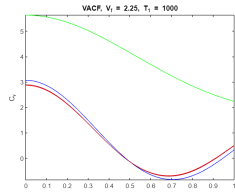
(f) $T = 300\text{K}$, $V_f = 6.75$

Figure: MSD as a function of time (τ_1) depicted by $\text{MSD} - \tau_1$ plots for four active Brownian particles with different masses in a microchannel with Poiseuille flow, under varying non-dimensional flow speeds and temperatures. The plots colored red, green, blue, and dark red correspond to the non-inertial particle and particles with masses of $1.5 \times 10^{-8} \text{ kg}$ (Inertial S1), $1.5 \times 10^{-9} \text{ kg}$ (Inertial S2), and $1.5 \times 10^{-10} \text{ kg}$ (Inertial S3), respectively, initial condition: $(X_0, Y_0) = (0, 0)$.

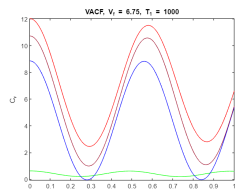
Velocity autocorrelation function (VACF): $\theta_0 = \pi/6$



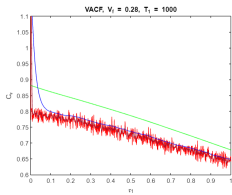
(a) $T = 0\text{K}$, $V_f = 0.28$



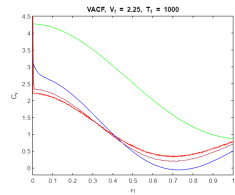
(b) $T = 0\text{K}$, $V_f = 2.25$



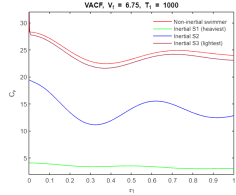
(c) $T = 0\text{K}$, $V_f = 6.75$



(d) $T = 300\text{K}$, $V_f = 0.28$



(e) $T = 300\text{K}$, $V_f = 2.25$



(f) $T = 300\text{K}$, $V_f = 6.75$

Figure: VACF (C_v) as a function of time (τ_1) depicted by $C_v - \tau_1$ plots for four active Brownian particles with different masses in a microchannel with Poiseuille flow, under varying non-dimensional flow speeds and temperatures. The plots colored red, green, blue, and dark red correspond to the non-inertial particle and particles with masses of $1.5 \times 10^{-8} \text{ kg}$ (Inertial S1), $1.5 \times 10^{-9} \text{ kg}$ (Inertial S2), and $1.5 \times 10^{-10} \text{ kg}$ (Inertial S3), respectively, initial condition: $(X_0, Y_0) = (0, 0)$.

Joint probability distribution function (JPDF): $V_f = 0.28$

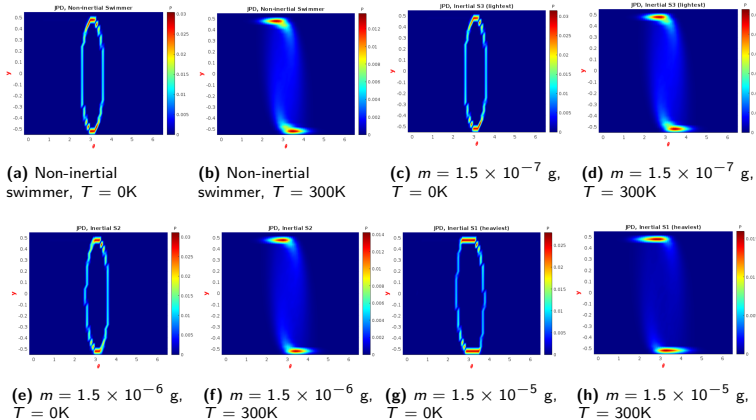


Figure: JPDF, $P(\theta, Y)$, plots of four spherical self-propelled particles with different inertial parameters in a microchannel with Poiseuille flow having non-dimensional flow speed, $V_f = 0.28$, at two different temperatures, $T = 0\text{K}$ (noise-free dynamics) and $T = 300\text{K}$ (dynamics with noise); initial conditions $(X_0, Y_0, \theta_0) = (0, 0, \pi/6)$.



JPDF: $V_f = 2.25$

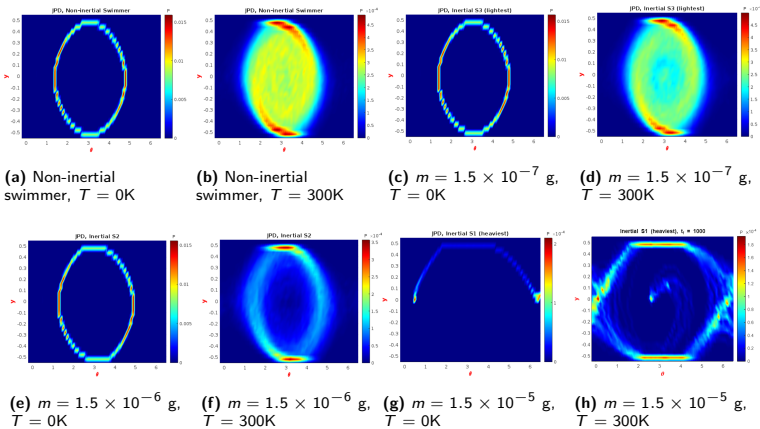
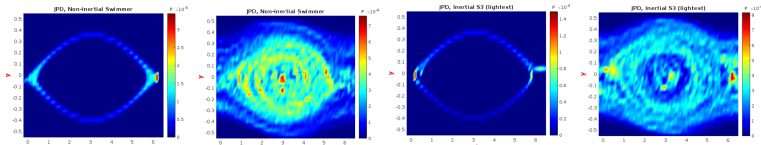


Figure: JPDF, $P(\theta, Y)$, plots of four spherical self-propelled particles with different inertial parameters in a microchannel with Poiseuille flow having non-dimensional flow speed, $V_f = 2.25$, at two different temperatures, $T = 0\text{K}$ (noise-free dynamics) and $T = 300\text{K}$ (dynamics with noise); initial conditions $(X_0, Y_0, \theta_0) = (0, 0, \pi/6)$.



JPDF: $V_f = 6.75$

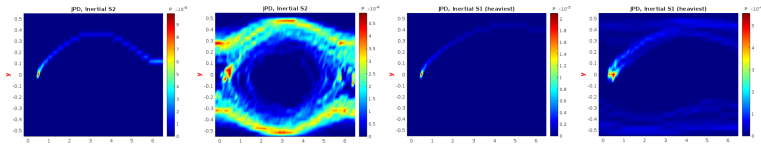


(a) Non-inertial swimmer, $T = 0\text{K}$

(b) Non-inertial swimmer, $T = 300\text{K}$

(c) $m = 1.5 \times 10^{-7} \text{ g}$, $T = 0\text{K}$

(d) $m = 1.5 \times 10^{-7} \text{ g}$, $T = 300\text{K}$



(e) $m = 1.5 \times 10^{-6} \text{ g}$, $T = 0\text{K}$

(f) $m = 1.5 \times 10^{-6} \text{ g}$, $T = 300\text{K}$

(g) $m = 1.5 \times 10^{-5} \text{ g}$, $T = 0\text{K}$

(h) $m = 1.5 \times 10^{-5} \text{ g}$, $T = 300\text{K}$

Figure: JPDF, $P(\theta, Y)$, plots of four spherical self-propelled particles with different inertial parameters in a microchannel with Poiseuille flow having non-dimensional flow speed, $V_f = 6.75$, at two different temperatures, $T = 0\text{K}$ (noise-free dynamics) and $T = 300\text{K}$ (dynamics with noise); initial conditions $(X_0, Y_0, \theta_0) = (0, 0, \pi/6)$.



References

- [1] Narender Khatri and PS Burada. Diffusion of chiral active particles in a poiseuille flow. *Physical Review E*, 105(2):024604, 2022.
- [2] Andreas Zöttl and Holger Stark. Nonlinear dynamics of a microswimmer in poiseuille flow. *Physical review letters*, 108(21):218104, 2012.
- [3] Kai Qi, Hemalatha Annapu, Gerhard Gompper, and Roland G Winkler. Rheotaxis of spheroidal squirmers in microchannel flow: Interplay of shape, hydrodynamics, active stress, and thermal fluctuations. *Physical Review Research*, 2(3):033275, 2020.
- [4] Andreas Zöttl. Hydrodynamics of microswimmers in confinement and in poiseuille flow. 2014.
- [5] Akash Choudhary, Subhechchha Paul, Felix Rühle, and Holger Stark. How inertial lift affects the dynamics of a microswimmer in poiseuille flow. *Communications Physics*, 5(1):1–9, 2022.
- [6] Shiyang Wang and AM Ardekani. Unsteady swimming of small organisms. *Journal of Fluid Mechanics*, 702:286–297, 2012.
- [7] Amandine Hamel, Cathy Fisch, Laurent Combettes, Pascale Dupuis-Williams, and Charles N Baroud. Transitions between three swimming gaits in paramecium escape. *Proceedings of the National Academy of Sciences*, 108(18):7290–7295, 2011.
- [8] S Wang and A Ardekani. Inertial squirmer. *Physics of Fluids*, 24(10):101902, 2012.
- [9] Aditya S Khair and Nicholas G Chisholm. Expansions at small reynolds numbers for the locomotion of a spherical squirmer. *Physics of Fluids*, 26(1):011902, 2014.
- [10] Christian Scholz, Soudeh Jahanshahi, Anton Ldov, and Hartmut Löwen. Inertial delay of self-propelled particles. *Nature communications*, 9(1):1–9, 2018.
- [11] Hartmut Löwen. Inertial effects of self-propelled particles: From active brownian to active langevin motion. *The Journal of chemical physics*, 152(4):040901, 2020.
- [12] Huaijuan Zhou, Carmen C Mayorga-Martinez, Salvador Pané, Li Zhang, and Martin Pumera. Magnetically driven micro and nanorobots. *Chemical Reviews*, 121(8):4999–5041, 2021.
- [13] Liqiang Ren, Nitesh Nama, Jeffrey M McNeill, Fernando Soto, Zhifei Yan, Wu Liu, Wei Wang, Joseph Wang, and Thomas E Mallouk. 3d steerable, acoustically powered microswimmers for single-particle manipulation. *Science advances*, 5(10):eaax3084, 2019.
- [14] Amirreza Aghakhani, Oncay Yasa, Paul Wrede, and Metin Sitti. Acoustically powered surface-slipping mobile microrobots. *Proceedings of the National Academy of Sciences*, 117(7):3469–3477, 2020.
- [15] EA Lisin, OS Vaulina, II Lisina, and OF Petrov. Motion of a self-propelled particle with rotational inertia. *Physical Chemistry Chemical Physics*, 24(23):14150–14158, 2022.
- [16] Christina Kurzthaler and Howard A Stone. Microswimmers near corrugated, periodic surfaces. *Soft matter*, 17(12):3322–3332, 2021.

